# *Heme oxygenase-1 expression in human gliomas and its correlation with poor prognosis in patients with astrocytoma*

**Norberto A. Gandini, María E. Fermento, Débora G. Salomón, Diego J. Obiol, Nancy C. Andrés, Jean C. Zenklusen, Julián Arevalo, et al.**

**Tumor Biology**
Tumor Markers, Tumor Targeting and Translational Cancer Research

ISSN 1010-4283

Tumor Biol.
DOI 10.1007/s13277-013-1373-z

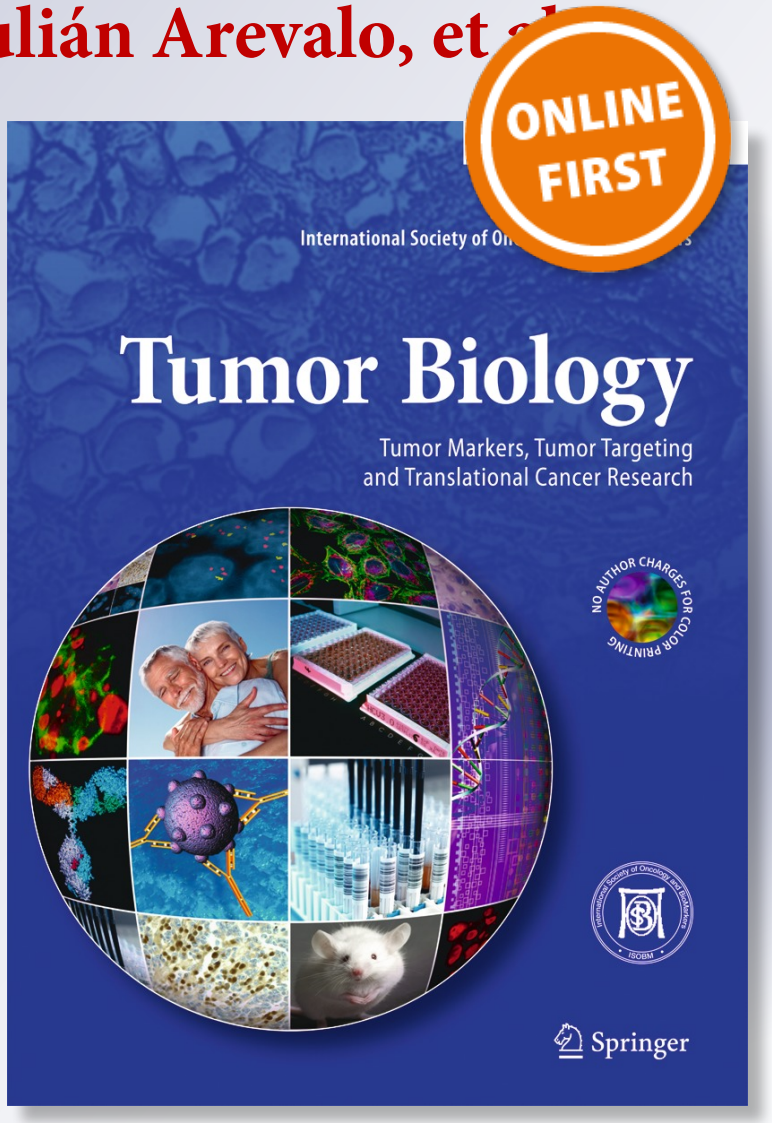


Springer

Tumor Biol.
DOI 10.1007/s13277-013-1373-z

RESEARCH ARTICLE

# Heme oxygenase-1 expression in human gliomas and its correlation with poor prognosis in patients with astrocytoma

**Norberto A. Gandini · María E. Fermento · Débora G. Salomón · Diego J. Obiol · Nancy C. Andrés · Jean C. Zenklusen · Julián Arevalo · Jorge Blasco · Alejandro López Romero · María M. Facchinetti · Alejandro C. Curino**

Received: 5 August 2013 / Accepted: 28 October 2013


**Abstract** In human glioma tumors, heme oxygenase-1 (HO-1) has been shown to be upregulated both when compared with normal brain tissues and also during oligodendroglioma progression. The cell types that express HO-1 have been shown to be mainly macrophages/microglia and T cells. However, many other reports also demonstrated that cell lines derived from glioma tumors and astrocytes express HO-1 after the occurrence of a wide variety of cell injuries and stressors. In addition, the significance of HO-1 upregulation in glioma had not, so far, been addressed. We therefore aimed at investigating the expression and significance of HO-1 in human glial tumors. For this purpose, we performed a wide screening of HO-1 expression in gliomas by using tissue microarrays containing astrocytomas, oligodendrogliomas, mixed tumors, and normal brain tissues. We subsequently correlated protein expression with patient clinicopathological data. We found differences in HO-1 positivity rates between non-malignant brain (22 %) and gliomas (54 %, $p=0.01$). HO-1 was expressed by tumor cells and showed cytoplasmic localization, although 19 % of tumor samples also depicted nuclear staining. Importantly, a significant decrease in the overall survival time of grade II and III astrocytoma patients with HO-1 expression was observed. This result was validated at the mRNA level in a cohort of 105 samples. However, no association of HO-1 nuclear localization with patient survival was detected. In vitro experiments aimed at investigating the role of HO-1 in glioma progression showed that HO-1 modulates glioma cell proliferation, but has no effects on cellular migration. In conclusion, our results corroborate the higher frequency of HO-1 protein expression in gliomas than in normal brain, demonstrate that HO-1 is expressed by glial malignant cells, and show an association of HO-1 expression with patients' shorter survival time.

**Keywords** Heme oxygenase-1 · Glioma · Survival · Tissue microarray

**Electronic supplementary material** The online version of this article (doi:10.1007/s13277-013-1373-z) contains supplementary material, which is available to authorized users.

N. A. Gandini · M. E. Fermento · D. G. Salomón · D. J. Obiol · N. C. Andrés · M. M. Facchinetti · A. C. Curino (✉)
Laboratorio de Biología del Cáncer, Instituto de Investigaciones Bioquímicas Bahía Blanca (INIBIBB-CONICET), Camino La Carrindanga Km 7, 8000 Bahía Blanca, Argentina
e-mail: acurino@criba.edu.ar

J. C. Zenklusen
The Cancer Genome Atlas Program Office, National Cancer Institute, National Institutes of Health, Bethesda, MD, USA

J. Arevalo · J. Blasco
Servicio de Patología del Hospital Interzonal de Agudos Dr. José Penna, Bahía Blanca, Argentina

A. López Romero
Laboratorios IACA, Bahía Blanca, Argentina

## Introduction

Tumors of the central nervous system include a number of unique, often difficult to treat neoplasms, being the tumors of glial origin, gliomas the most common intracranial neoplasia in adults. The highly invasive nature of this tumor prevents complete tumor resection and causes significant neurologic morbidity and mortality [1]. Current treatment for gliomas remains suboptimal, and the promise for improved therapies rests largely on a better understanding of the underlying biology and genetics of these tumors [2]. The molecular and genetic heterogeneity of gliomas undoubtedly contributes to

Published online: 15 November 2013

this suboptimal response to treatment that is usually based on standard pathologic diagnoses [3–5]. Thus, glioma diagnosis has been historically based on examining the cellular morphology of the tumor to assess its presumed cell of origin and surrogate markers of tumor aggressiveness (necrosis, nuclear pleomorphism, mitoses) to determine the tumor grade [6]. However, these tumor characteristics are insufficient to predict the evolution of each individual patient; for example, within identical histological grade tumors, there can be found distinct biological subtypes characterized by different prognostic factors [7]. Therefore, it is important to find tumor markers able to differentiate subtypes of malignant gliomas. The majority of genetic or epigenetic alterations described in gliomas have been found in the epidermal growth factor receptor, platelet-derived growth factor receptor, murine double minute 2, cyclin-dependent kinase 4 and 6, cyclin-dependent kinase inhibitor 2A, tumor suppressor protein p53, retinoblastoma 1, phosphatase and tensin homolog, $O^6$-alkylguanine DNA alkyltransferase, and isocitrate dehydrogenase (NADP) cytoplasmic (IDH1) genes [8, 9]. Targeted therapies directed to some of these ubiquitous cancer-associated targets (i.e., erlotinib and gefitinib) have unfortunately met with limited success [10, 11], further reinforcing the need for the identification of glioma-specific novel molecular targets.

Heme oxygenase (HO) is a microsomal enzyme which catalyzes the first rate-limiting step in the degradation of heme, yielding equimolar quantities of biliverdin, carbon monoxide (CO), and iron [12–14], thus removing this potent pro-oxidant and pro-inflammatory agent. It has recently been recognized that these three products have important physiological roles [14–16]. Two distinct mammalian HO isoforms (HO-1 and HO-2) have been identified. HO-1, the inducible 32-kDa isoform, is a ubiquitous heat shock protein (HSP32) [17]. HO-1 can be induced in response to cellular stress oxidative stimuli and hypoxia, an important process frequently occurring during tumoral growth. In contrast, HO-2 is a constitutively expressed 36-kDa protein [18]. Regarding brain physiology, both neuronal and non-neuronal brain cells exhibit a capacity to rapidly upregulate HO-1 in response to noxious stimuli [19, 20], and this upregulation has been shown to promote both neuroprotection and neuronal dysfunction [20].

An increasing body of evidence indicates that HO-1 also plays an important role in cancer. It has been suggested that eight hallmark capabilities and two enabling characteristics are necessary for a complete tumor formation and progression. The first eight capabilities are: sustaining proliferative signaling, evading growth suppressors, resisting cell death, enabling replicative immortality, inducing angiogenesis, reprogramming of energy metabolism, evading immune destruction, and activating invasion and metastasis. The enabling characteristics are genome instability and inflammation [21, 22]. There is evidence of HO-1 being related to most of these capabilities and the two enabling characteristics [14, 18]. Furthermore, HO-1 was reported to be upregulated in the majority of the rat, mouse, and human tumors analyzed [14, 18]. In this regard, we have recently demonstrated that HO-1 is upregulated in squamous cell carcinoma and that its nuclear expression increases with tumor progression [23]. We have also shown that it is overexpressed in non-small cell lung cancer [24]. Elevated HO-1 mRNA expression has been observed in brain tumors when compared to normal brains [25], and an increase in HO-1 protein expression with oligodendroglioma progression [26] and with tumor grade [27] was also demonstrated. However, these studies were performed on a small number of human tumor samples, the enzyme being mostly detected in macrophages/microglia [26, 28] or T cells [27], and no correlation with survival data was performed. For these reasons, one of the objectives of this study was to investigate the expression of HO-1 in a large collection of glioma samples by immunohistochemistry on tissue microarrays (TMAs), evaluating the tumor cell type expressing HO-1 and analyzing the relationship between HO-1 expression and overall survival rate.

Interestingly, HO-1 has been detected in the nucleus of mouse cell lines after exposure to hemin and hypoxia, showing that this localization is linked to the upregulation of genes that protect against oxidative stress [29]. Furthermore, it has been recently reported that HO-1 nuclear localization is associated with human prostate [30] and head and neck [23] cancer progression and with imatinib resistance in myeloid leukemia cells [31]. It is also important to mention that L-glutamate has been shown to induce the nuclear translocation of HO-1 in primary cultured rat astrocytes [32]. In light of these results, another objective of this study was to investigate the incidence of nuclear localization of HO-1 in human glioma samples.

## Materials and methods

### Patients and tumors

Glioma tumor samples were obtained from the Glioma Biorepository at Henry Ford Hospital, Detroit, MI, and data are deposited at the US National Cancer Institute repository for Molecular Brain Neoplasia Data (REMBRANDT). The REMBRANDT database [33] (National Cancer Institute, 2005; http://rembrandt.nci.nih.gov, accessed 15 October 2013) is provided as a public service by the Neuro-Oncology Branch of the National Cancer Institute (NCI) and the National Institute of Neurological Disorders and Stroke (NINDS). It contains many samples of brain tumors and non-malignant brains, including the ones that are part of the tissue microarray used in the present investigation and the sample data used for the multivariate analysis. All tumor samples were obtained with written consent in accordance with institutional guidelines. Tumor samples included astrocytomas

(WHO grades II and III (ASTRO) and WHO grade IV glioblastoma multiforme (GBMs)), oligodendroglioma (ODG), oligoastrocytoma (MIXED), and also non-malignant brain tissues obtained from epilepsy surgery. All tissue specimens were obtained at initial diagnosis from untreated patients and by resection or by biopsy and were morphologically classified and graded according to the current WHO system. The follow-up period lasted a median (Md) of 19 months, with a range of 0.03–144.88 months. From these samples, 116 were used to construct the tissue microarrays. From these 116, five samples were also used to obtain mRNA for RT-qPCR studies. Also, data of HO-1 mRNA expression from a cohort of 105 ASTRO samples were used for the multivariate studies.

Additionally, a cohort of eight independent glioma tissue samples was analyzed in this retrospective study. These were retrieved from the Pathology Service of a regional hospital with IRB approval and were staged according to the American Joint Committee on Cancer Staging System [34]. They belonged to patients who had undergone surgical treatment between 1994 and 2007. These samples were ASTRO (grade II, $n=4$; grade III, $n=2$), ODG (grade III, $n=1$), and GBM (grade IV, $n=1$).

## Tissue microarray construction

TMAs were constructed at the Neuro-Oncology Branch of the NCI/NINDS with IRB approval. Two different array blocks were used. Both blocks included a total of 116 glioma cases with varying degrees of differentiation (ODG, $n=29$; ASTRO, $n=18$; MIXED, $n=12$; and GBM, $n=57$). Additionally, 18 cores of non-malignant brain tissues and 16 several other tissues (liver, colon, salivary gland, spleen, testis, lung, muscle, and kidney) were included as controls. Data on the initial diagnosis, staging, gender, and survival were collected. The distribution of cases based on their differentiation was similar; approximately 31 % of the cases were grade II, 20 % were grade III, and 49 % were grade IV. Three TMA slides of each array block were used for HO-1 immunostaining.

## Immunohistochemical staining

Immunohistochemical (IHC) staining was performed as previously described [35]. In brief, slides were deparaffinized in xylene and rehydrated in a series of ethanol dilutions (100, 96, and 70 %) and phosphate-buffered saline (PBS). They were incubated in 3 % hydrogen peroxide to quench endogenous peroxidase. After washing in PBS, sections were blocked in 2 % bovine serum albumin (BSA) in PBS (blocking solution). Sections were then incubated overnight at 4 °C with primary rabbit anti-HO-1 antibody (dilution, 1:200; SPA-896 Stressgen Bioreagents, Canada) followed by incubation with diluted biotinylated secondary antibody and then incubation with VECTASTAIN ABC Reagent (Vector Laboratories Inc.). For negative controls, the slides were subjected to the same IHC process, except that the primary antibody was omitted. Diaminobenzidine/$H_2O_2$ was used as a substrate for the immunoperoxidase reaction. They were lightly counterstained with hematoxylin, dehydrated through graded ethanol and xylene, and mounted with Permount (Fisher Scientific) for analysis by bright-field microscopy.

## Histopathological evaluation of staining intensities

TMA and individual slides were further reevaluated by the pathologists (JA and JB) to confirm diagnosis. Then, the immunostained sections were scored semi-quantitatively basing the procedure upon the proportion of cells stained and the staining intensity, as previously described [23]. In brief, the specimens were assessed using the semi-quantitative immunoreactive score (IRS). The IRS was calculated by multiplying the staining intensity (graded as 0=no, 1=weak, 2=moderate, and 3=strong staining) and the percentage of positively stained cells (0=less than 10 % of stained cells, 1=11–50 % of stained cells, 2=51–80 % of stained cells, and 3=more than 81 % of stained cells). Only representative tissue cores containing at least 200 tumor cells were scored. To estimate the discriminative value of the IRS for HO-1 expression in glioma, receiver operating characteristic (ROC) curves were plotted and the corresponding areas under the curve (AUC) were compared using various possible cutoff values, as described elsewhere [36]. The AUC in the model with IRS=1 was 0.658 (95% CI=0.55–0.77), with a sensitivity of 55.2 % and a specificity of 77.8 % for the point closest to [0.0, 1.0]; the AUC in the model with IRS=2 was 0.567 (95% CI=0.47–0.66), with a sensitivity of 29.3 % and a specificity of 83.3 % for the point closest to [0.0, 1.0] ($p=0.0075$ for the difference of the AUCs). Based on the area under the ROC curve values, the best cutoff value was determined as IRS=1. Values of IRS≥1 were considered to display positive expression of HO-1. All scores were entered into a standardized electronic spreadsheet (Excel for Microsoft Windows).

## RNA preparation and real-time RT-PCR

Total RNA was isolated from fresh brain tumor samples (glioblastomas, astrocytomas, and oligodendrogliomas) using an RNeasy Lipid Tissue Mini RNA Isolation Kit (Qiagen Science, MD) following the manufacturer's instructions. The quality of the RNA samples was determined by measuring the absorbance of RNA samples at 260 nm as well as by electrophoresis through agarose gels and staining with ethidium bromide. The 18S and 28S RNA bands were visualized under ultraviolet lighting. Reverse transcription of RNA was done in a final volume of 20 μl containing 13 RT-PCR buffer (500 mM each of deoxynucleotide triphosphate, 3 mM

$MgCl_2$, 75 mM KCl, 50 mM Tris–HCl, pH 8.3), 10 U RNasin RNase inhibitor (Promega Corp., Madison, WI), 10 mM DTT, 50 U Superscript II RNase H2 reverse transcriptase (Life Technologies, Inc., Gaithersburg, MD), 1.5 mM random hexamers (Pharmacia, Uppsala, Sweden), and 1 μg of total RNA. The samples were incubated at 20 °C for 10 min and 42 °C for 30 min, and reverse transcriptase was inactivated by heating at 99 °C for 5 min and cooling at 5 °C for 5 min. mRNA expression levels were quantified in triplicates by real-time RT-PCR on an ABI Prism 7900 sequence detection system (Applied Biosystems, Foster City, CA). The relative amount of target transcripts quantified by the standard curve method was normalized to the amount of human GAPDH transcripts found in the same sample. Primers and probes were purchased from Applied Biosystems (GAPDH: Hs03929097g1; HO-1: Hs01110250m1).

### Immunofluorescence analysis

Immunofluorescence was performed as previously described [23]. In brief, human glioma cell lines U87MG and T98G were routinely maintained in Dulbecco's modified Eagle's medium (Invitrogen, CA) supplemented with 10 % fetal bovine serum (Bioser, Argentina), 2 mM glutamine, 50 U/mL penicillin, and 0.05 mg/mL streptomycin. They were plated on glass coverslips, then fixed with 4 % paraformaldehyde in PBS, and permeabilized with 0.1 % triton X-100 in PBS for 10 min, followed by incubation with blocking solution (1 % BSA in PBS). The antibody employed for HO-1 staining was the rabbit anti-HO-1 antibody (dilution 1:400; SPA-896, Stressgen Bioregents, Canada); for F-actin staining, rhodamine phalloidin (1:1,000; R415 Molecular Probes, Invitrogen) was used. After incubation with the primary antibody, cells were incubated with anti-rabbit Alexa 566 fluoro-conjugated antibodies (Molecular Probes, Invitrogen). The coverslips were washed with PBS and then mounted on slides with Prolong Gold anti-fade reagent (Invitrogen). Images were captured with a Leica TCS SP2 confocal system (Heidelberg, Germany).

### Stable overexpression of HO-1 in T98G human glioblastoma cell line

The expression plasmids used (pcDNA3-HO-1 and pcDNA3-CTRL) were kindly donated by Dr. Elba Vazquez (Department of Biological Chemistry, University of Buenos Aires). The T98G cells were plated in 10-cm dishes at a density of $1 \times 10^6$ cells; the transfection procedure was performed the following day using Lipoafectamine (Invitrogen) according to the manufacturer's instructions. Stable transfectants (T98-HO-1 and T98-CTRL) were selected by incubating cells with G418 (40 mg/mL) for a period of 25 days. Overexpression of HO-1 was studied by immunoblotting.

### Immunoblotting

U87MG and T98G were seeded and grown sub-confluent until treatment with hemin 20 μM or vehicle (0.4 mL of NaOH 0.5 N and 0.5 mL Tris–HCl 0.5 N). Also, T98-HO-1 and T98-CTRL were seeded and grown sub-confluent. Immunoblotting was performed as described previously [34]. Briefly, 50 μg of protein (30 μg for the T98-HO-1 and T98-CTRL) was electrophoretically resolved by SDS-PAGE and transferred onto a polyvinylidene difluoride membrane Immobilon-P (Millipore, Bedford, MA). Blots were incubated with the same HO-1 polyclonal antibody used for IHC (1.5 mg/mL in PBS), and reactions were detected using horseradish peroxidase-conjugated secondary antibodies (1:5,000; Amersham Biosciences, Arlington Heights, IL) and enhanced chemiluminescence following the manufacturer's directions (Amersham, ECL Plus Western Blotting Detection Reagents, GE Healthcare, UK). Films were exposed 20 min for the detection of HO-1 in the blots, demonstrating the specificity of the antibody.

### Effects of HO-1 on cell viability and proliferation

The T98-HO-1 and T98-CTRL cells were plated at a density of 2,000 cells/well into 96-multi-well dishes in complete medium. The T98G cells were treated with 80 μM of hemin or vehicle for 48 h. Cell viability was measured by counting cells using a hemocytometer. The experiment was repeated three times and performed in quadruplicate.

In order to investigate HO-1 effects on cell proliferation, a 5-bromo-2-deoxyuridine (BrdU) proliferation assay was performed. Briefly, T98G cells were seeded in a 35-mm culture plate so as to attain 50–70 % confluence within 24 h, followed by treatment with hemin (80 μM) and SnPP (15 μM) or their respective vehicles for 48 h. The proliferative potential of treated cells was assessed by using the BrdU Proliferation Assay Kit (Becton Dickinson Immunocytometry Systems) following the manufacturer's instructions.

Additionally, T98-HO-1 and T98-CTRL cells were seeded in 35-mm Petri dishes and cultured until 80 % confluence. The cells were trypsinized, fixed with ice-cold 70 % ethanol, stained with propidium iodide (Roche), and analyzed for DNA content with FACScan flow cytometry (Becton Dickinson, Heidelberg, Germany). Data were analyzed using Cell Quest software (Becton Dickinson). At least 100,000 cells were analyzed for each sample.

The percentage of apoptotic cells was measured with flow cytometry following annexin V (FL1-H) and propidium iodide (PI; FL2-H) labeling. Briefly, T98G, T98-HO-1, and T98-CTRL cells were seeded in 35-mm Petri dishes and cultured until 80 % confluence. A minimum of $5 \times 10^5$ cells/mL were analyzed for each sample. Cells were washed in PBS and resuspended in binding buffer (1×, 5 μL). Annexin V-

FITC was added to 400 μL of cell suspension and then the apoptotic cells were counted using FACScan flow cytometry (Becton Dickinson). All these experiments were carried out in triplicate and were repeated twice.

### Effects of HO-1 on cell migration

Cell migration was studied by employing the "wound healing" assay [37]. Briefly, T98G, T98-HO-1, and T98-CTRL cells were seeded in 35-mm Petri dishes and cultured until confluence. T98G cells were treated with vehicle or hemin 80 μM for 24 h. The cells were then scraped with a 200-μL micropipette tip and monitored at 0, 8, and 24 h. The uncovered wound area was measured and quantified at different intervals with ImageJ 1.37v (NIH).

### Statistical analysis

The statistical significance of HO-1 expression levels and rate between groups was determined using the Mann–Whitney $U$ and the $\chi^2$ tests, respectively. Survival intervals were measured from the time of surgery to death from disease or until the last follow-up. Overall survival according to HO-1 expression was constructed using Kaplan–Meier survival curves, and the log-rank test was used for the comparison of survival curves in univariate analyses.

Multivariate analysis was performed in the cohort of 105 astrocytoma cases for the studies of HO-1 mRNA expression using the stepwise Cox proportional hazards model. The variables included in the model were age (<50 or >50), gender, tumor grade, Karnofsky performance status (<80 or >80), and HO-1 mRNA levels (high and low). ROC curve analysis was used to determine the cutoff value for high HO-1 mRNA expression. In the HO-1 score, the sensitivity and the specificity for patient outcome (death due to disease or censored) were plotted, thus generating ROC curves. The ROC curve (AUC= 0.705, 95% CI=0.61–0.79) clearly showed the point closest to [0.0, 1.0] which maximizes both sensitivity and specificity for the outcome (sensitivity=54.4 %, specificity=75.68 %). The point was selected as the cutoff value. The tumors designated as "high-expression" tumors were those with scores above the value. All variables were entered in the multivariate analysis as categorical ones. All patients received the same treatment after surgery. $T$ test was used to determine statistical significance between sample sets in the cellular proliferation and migration studies.

All analyses were performed using GraphPad Prism 5.01 for Windows and MedCalc Statistical Software version 12.7.4. Values of $p<0.05$ indicated a significant result.

## Results

### Validation of antibody for immunohistochemical staining and study of the patterns of HO-1 expression in individual glioma samples

As already described, previous studies demonstrated that HO-1 mRNA increases in tumors when compared to normal brain [25] and that HO-1 protein increases with oligodendroglioma progression [26] and tumor grade [27], albeit all of them used a small number of samples. Therefore, we aimed at studying HO-1 expression in a larger collection of tumor samples, and for this purpose, we performed immunohistochemical staining for HO-1 in glioma tissue microarrays (TMAs). To validate the use of the antibody for detection of HO-1 in human glioma samples, we first performed Western blot of protein lysates of human glioblastoma multiforme cell lines (T98G and U87MG). As shown in Fig. 1a, the antibody recognized only one band representing a protein with the molecular weight of HO-1 (32 kDa). Basal HO-1 levels were high (lanes 1 and 3) and hemin treatment increased even more the expression of the protein in these cells (lanes 2 and 4), further demonstrating that the protein detected by the antibody is HO-1.

Tissue microarrays allow the screening of molecules in a large collection of normal and tumor tissues simultaneously, a task which would be tedious with conventional molecular pathology technologies. However, the qualitative information concerning patterns of expression in tumor cells and tissues that can be obtained with TMAs is limited. We therefore examined the distribution of HO-1 in individual paraffin-embedded tissue sections obtained from surgically resected biopsies. Furthermore, the analysis of these tumors was useful to set up the optimal conditions and further validate the use of this antibody for immunohistochemical staining. In total, eight glioma samples included in paraffin blocks were assessed for HO-1 protein expression, and serial sections were stained with an antibody to glial fibrillary acidic protein (GFAP) to evaluate whether the morphology of the cells expressing HO-1 is similar to that of the cells expressing GFAP. This analysis showed that HO-1 displayed strong cytoplasmic staining in cells with the morphology of astrocytes (Fig. 1b, right picture) compared with no staining when the primary antibody was omitted (Fig. 1b, left picture). As described in the "Introduction," nuclear localization of HO-1 was recently described in various types of tumors. Therefore, we studied HO-1 subcellular localization in these glioma tissues. We detected that some of the tumors (3/8, 37 %) showed nuclear expression of the protein (mean percentage of stained nuclei of all the positive samples, 15±5 %). In order to further confirm that malignant astrocytes express HO-1, we also analyzed HO-1 expression patterns in glioma cell lines by immunofluorescence and observed that HO-1 was highly expressed and localized in both the cytoplasm and nuclei in

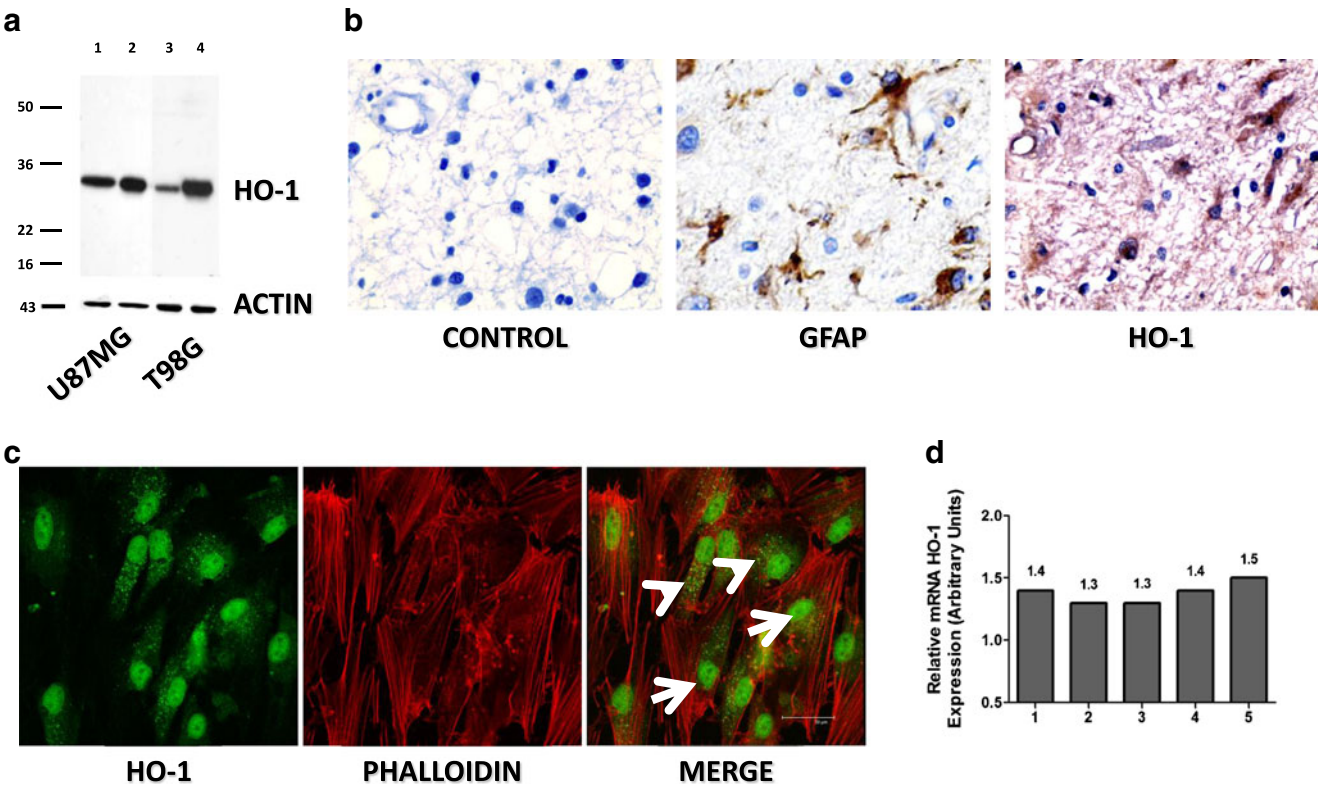


**Fig. 1** HO-1-specific detection in human gliomas. **a** Western blot showing one band with the molecular weight of HO-1. T98G and U87MG cells were treated with hemin (20 μM) or vehicle, lysed, and immunoblotted against HO-1, as explained in "Materials and methods." Basal levels of HO-1 (*lanes 1* and *3*) or hemin-induced HO-1 (*lanes 2* and *4*) are shown. Actin expression was used as a loading control. The electrophoretic mobilities of marker proteins are indicated to the *left*. **b** Immunohistochemistry for HO-1 in human glioma samples. Negative control showing the absence of staining (*left picture*). Representative IHC showing GFAP staining in an astrocytoma (*middle picture*) and HO-1 staining in a consecutive section (*right picture*), at ×400 magnifications. **c** Immunofluorescence for HO-1 in T98G cells. *Arrows* show nuclear expression of the protein. *Arrowheads* indicate cytoplasmic expression of HO-1 in T98G. Similar results were observed in U87MG line (data not shown). Original magnification, ×630. **d** Detection of HO-1 mRNA by qRT-PCR in fresh glioma tissues isolated from different patients of TMA. *1–3*, WHO III astrocytomas; *4*, WHO II oligodendroglioma; *5*, WHO II astrocytoma

T98G (Fig. 1c). Similar results were observed in the U87MG cell line (data not shown).

In order to confirm the expression of HO-1 by a different and independent method, mRNA was extracted from fresh samples of human gliomas and HO-1 was analyzed using quantitative real-time PCR. As shown in Fig. 1d, HO-1 was specifically detected in all glioma samples.

Taken together, these analyses showed that malignant astrocytes also express HO-1 and that this expression was observed in the cytoplasm and nucleus. They also showed that HO-1 could be specifically detected with IHC and by RT-qPCR in human glioma tissues and by Western blot and immunofluorescence in human glioma cell lines. This antibody was used for further studies of HO-1 expression on TMAs.

## HO-1 expression in human glioma TMAs

Table 1 shows the characteristics of the studied population. The expression of HO-1 in non-malignant brain tissue sections was mostly negative (14/18; Fig. 2a), with few positive samples (4/18) displaying low levels of HO-1.

Furthermore, significant differences between gliomas and non-malignant brain tissues in the incidence (54 and 22 % positive samples, respectively; $\chi^2$: $p=0.01$) and levels (median IRS=1.3 and 0.5, respectively; Mann–Whitney test: $p=0.02$) of HO-1 were observed. The distribution of cases according to IRS is shown in Fig. 2f; selected cases showing HO-1 expression and their IRS are shown in Electronic supplementary material (ESM) Online Resource 1. As described above, very recent reports described the nuclear localization of HO-1, including ours [23]. The subcellular analysis of the expression of HO-1 in tissue microarrays detected that some of the tumors (12/63, 19 %) showed nuclear expression of the protein, although the incidence was low (mean percentage of stained nuclei of all the positive samples, 15±5 %; Fig. 2b, c, red arrows). The majority of the samples showed cytoplasmic localization of HO-1 (Fig. 2d, e, red arrows). There were no significant differences in the rate of nuclear localization when comparing gliomas with non-malignant tissues ($p=0.93$).

**Table 1** Characteristics of the studied population

| | Normal | WHO II | WHO III | WHO IV |
|---|---|---|---|---|
| Cases (*n*) | 18 | 36 | 23 | 57 |
| Age (years), Md (range) | 37 (11–61) | 40 (15–74) | 41 (24–69) | 54.5 (19–78) |
| Gender | | | | |
| Male | 3 | 11 | 4 | 10 |
| Female | 4 | 5 | 7 | 7 |
| NA | 11 | 20 | 12 | 40 |
| Histopathologic type | | | | |
| ASTRO[a] | – | 8 | 10 | 57 |
| ODG | – | 24 | 5 | – |
| MIXED | – | 4 | 8 | – |
| Survival time, Md (range) | – | 42.21 (0.03–103.82) | 28.40 (0.23–75.71) | 14.79 (1.15–144.88) |

Survival time is expressed in months

*NA* not available, *Md* median

[a] WHO IV is GBM

## Association of HO-1 expression with clinicopathological parameters

Since different histological subtypes and grades of gliomas were included in the TMA, we investigated whether the expression was different among them. The specific analysis performed to compare each histologic subtype with non-malignant brain tissue showed significant differences in the incidence of expression of HO-1 in ODG ($p=0.008$) and ASTRO ($p=0.018$; Table 2).

Moreover, when comparing non-malignant brain tissues with WHO grade II ($p=0.012$), WHO grade III ($p=0.027$), and WHO grade IV ($p=0.033$), the HO-1 expression rates were also found increased. When analyzing the HO-1 expression levels, an increase was observed in the IRS of ODG ($p=0.006$), ASTRO ($p=0.048$), and WHO grades II ($p=0.013$) and III ($p=0.016$) when compared to the non-malignant brains (ESM Online Resource 2).

## Association of HO-1 expression with patients' overall survival

From a cohort of 95 patients who received the same therapeutic regimen after surgery, we performed an analysis of survival according to the Kaplan–Meier method. In univariate studies, we observed that the positive expression of HO-1 protein was

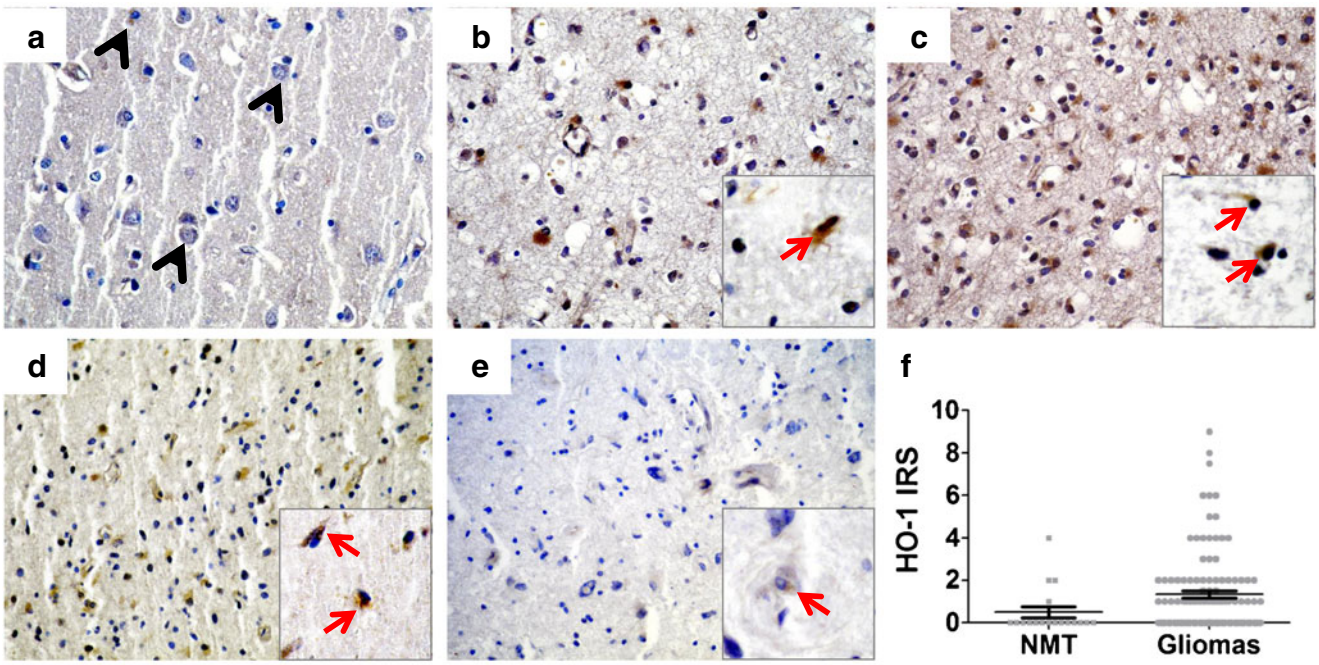


**Fig. 2** HO-1 expression in TMA. Photomicrographs of non-malignant brain tissue (**a**), ASTRO grade II (**b**), ODG (**c**), MIXED (**d**), and GBM (**e**). *Arrowheads* in (**a**) indicate the absence of HO-1 nuclear or cytoplasmic expression. *Red arrows* in (**b**) and (**c**) indicate cells with HO-1 nuclear expression. *Red arrows* in (**d**) and (**e**) indicate cells with HO-1 cytoplasmic expression. Original magnification of pictures, ×400 and ×1,000 for the *inset*. **f** Dot plot showing differences in HO-1 expression between glioma and non-malignant brain tissue

**Table 2** Association of HO-1 expression with some clinicopathological parameters

| Clinicopathological parameters | Cases, *n* | Negative, *n* (%) | Positive, *n* (%) | *p* value |
|---|---|---|---|---|
| Grade | | | | |
| Non-malignant | 18 | 14 (77.8) | 4 (22.2) | |
| WHO II | 36 | 15 (41.6) | 21 (58.4) | 0.012 |
| WHO III | 23 | 10 (43.5) | 13 (56.5) | 0.027 |
| WHO IV | 57 | 28 (49.1) | 29 (50.9) | 0.033 |
| Histological type | | | | |
| Non-malignant | 18 | 14 (77.8) | 4 (22.2) | |
| ASTRO[a] | 75 | 35 (46.7) | 40 (53.3) | 0.018 |
| ODG | 29 | 11 (37.9) | 18 (62.1) | 0.008 |
| MIXED | 12 | 7 (58.3) | 5 (41.7) | 0.255 |

HO-1 expression, as assessed by IHC performed in the glioma TMAs, was correlated with tumor grade and histological type. *p* values of $\chi^2$ test are shown

* GBM are included in the ASTRO group

not associated with overall survival when all glioma patients were analyzed jointly ($p=0.640$; Fig. 3a). As already mentioned, nuclear localization of HO-1 has been associated with tumor progression in other types of cancer; therefore, we evaluated whether this was also the case in gliomas. However, no association of nuclear HO-1 with patient survival was observed ($p=0.356$; Fig. 3b). Tumor grade is the most informative factor for stratification into subgroups with different prognoses, and glioblastoma has the worst prognosis, with a median overall survival of only 15 months. We therefore evaluated the association of HO-1 expression with the patients' overall survival for each histologic subtype, analyzing GBMs separately. The expression of HO-1 was not associated with the overall survival time of ODG ($n=21$, $p=0.943$; Fig. 4b), MIXED ($n=11$, $p=0.901$; Fig. 4c), or GBM ($n=50$, $p=0.247$; Fig. 4d) patients. Interestingly, HO-1 expression was associated with reduced survival time in patients with ASTRO ($n=13$, $p=0.036$; Fig. 4a). Since the number of samples in this subgroup of astrocytoma is small, a multivariate analysis is not possible. We therefore investigated the association of HO-1 mRNA expression with patient survival in a cohort of 105 astrocytoma samples of the REMBRANDT database. These samples were dichotomized into low- and high-gene-expression groups based on ROC curve analysis for patient outcome. Univariate analysis showed that a high expression of HO-1 was associated with shorter overall survival of patients ($p<0.001$; ESM Online Resource 3). Multivariate analysis using the Cox proportional hazards model identified age ($p<0.0001$), WHO grade ($p=0.0261$), and HO-1 levels ($p=0.0001$) as independent prognostic factors in overall survival in this cohort of astrocytomas (ESM Online Resource 3).

### *HO-1 effect on cellular proliferation and migration*

Since we observed that the expression of HO-1 in grade II and III astrocytoma patients' specimens was associated with shorter overall survival, we aimed at studying the underlying mechanisms that could potentially explain this association. For this purpose, we activated HO-1 in the human glioma cell line T98G both by hemin treatment and by stable overexpression of the enzyme and further performed analyses of cell viability. As shown in Fig. 5a, hemin significantly increases cell count when compared with the control group (43 %, $*p=0.036$). Also, HO-1-overexpressing cells (T98-HO-1) exhibited a similar increase in cell count when compared to control cells (T98-CTRL, $*p<0.0001$).

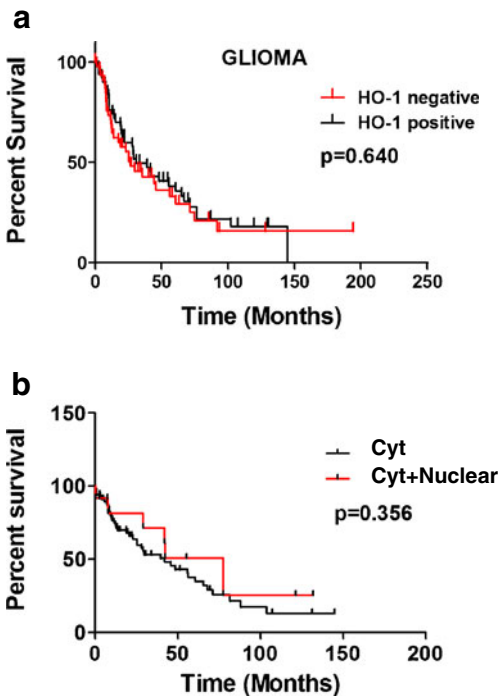


**Fig. 3** Correlation of HO-1 expression with patients' survival time in gliomas. Tumor sections of glioma patients ($n=95$) were divided into HO-1 positive and HO-1 negative (**a**) or into cytoplasmic and nuclear HO-1 (*Cyt+Nuclear*) and only cytoplasmic HO-1 (*Cyt*) (**b**) as determined by immunohistochemical evaluation. Kaplan–Meier survival analysis was performed. The log-rank test was used to determine significance between both survival curves

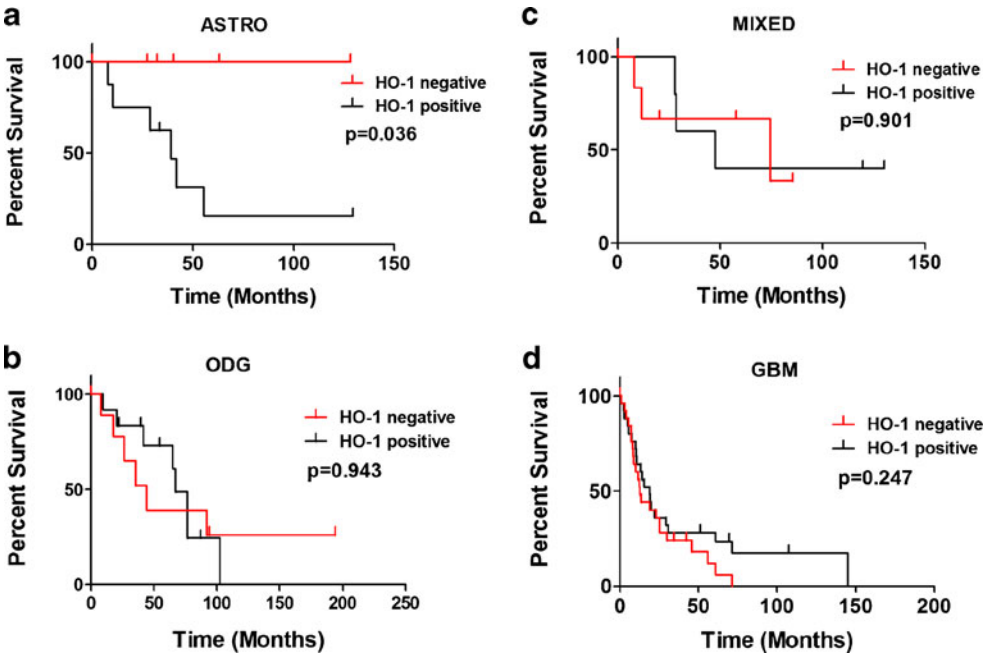


**Fig. 4** Correlation of HO-1 expression with patients' survival time in the various histologic subtypes. Tumor sections of ASTRO ($n=13$, $p=0.036$) (**a**); ODG ($n=21$, $p=0.943$) (**b**); MIXED ($n=11$, $p=0.901$) (**c**); and GBM ($n=50$, $p=0.247$) (**d**) were divided into HO-1 positive and HO-1 negative as determined by immunohistochemical evaluation. Kaplan–Meier survival analysis was performed. The log-rank test was used to determine significance between survival curves

In order to further analyze whether the observed increase in cell count could be due to a stimulation of cell proliferation, we did BrdU and propidium iodide staining followed by flow cytometry. As shown in Fig. 5b, HO-1 activation increases BrdU incorporation, whereas HO-1 inhibition decreases it. In addition, HO-1 genetic overexpression increases S phase cell population ($p=0.01$; Fig. 5c), whereas it has no effect on sub-$G_0/G_1$ cell population. In order to further corroborate that HO-1 had no effect on the apoptosis rate, we performed annexin V staining followed by flow cytometry. No differences in annexin V-positive cells were observed with HO-1 modulation (data not shown).

Infiltration throughout the brain is a prominent feature of low- and high-grade malignant gliomas usually involving the activation of several processes, including the migratory properties of the cells. Therefore, we analyzed the involvement of HO-1 on human glioma cellular migration by means of a wound closure assay. As shown in Fig. 5d, no differences were observed in the migratory rate of HO-1-overexpressing cells.

## Discussion

In this study, we have demonstrated that the incidence and levels of HO-1 expression are low in non-malignant human brain tissues and increase in glioma tissues. These results are coincident with previous studies of HO-1 expression in other types of cancer. Thus, HO-1 expression was reported to be strongly upregulated in the majority of the rat, mouse, and human tumors analyzed. This overexpression has been demonstrated in lymphosarcoma [38], prostate carcinoma [30, 39], brain tumors [25, 26], renal carcinoma [40], hepatoma [41], melanoma [42], Kaposi sarcoma [43], pancreatic cancer [44], chronic myeloid leukemia [45], and in oral squamous cell carcinoma [46–48]. Our group has also recently published that HO-1 is upregulated in head and neck squamous cell carcinoma [23] and in lung cancer [24]. In relation to brain tumors, our results are in agreement with a previous work showing the upregulation of HO-1 mRNA in human brain tumors [25] and with other reports showing an increase in enzyme expression with oligodendroglioma progression [26] and with tumor grade [27]. We have also shown that HO-1 is expressed mainly by tumor cells in the majority of human gliomas. However, contrary to our observations, the latter two reports mentioned showed that macrophages/microglia were the cell types mainly expressing HO-1. Similarly, Nishie and collaborators [28] reported that HO-1 protein was expressed by infiltrating T cells. Of note is that all these previous reports used a small number of samples, a fact which may limit the conclusions, and therefore it was deemed necessary to perform a wider study of HO-1 expression in these tumors. On the other hand, many neurodegenerative diseases such as Parkinson, Alzheimer, multiple sclerosis, cerebral infarcts, hemorrhages, and contusions have been shown to present an increased expression of HO-1 in glial cells [20], and HO-1 expression in brain tissues following induction by many agents has been demonstrated to occur mainly in glial cells [20]. Additionally, some reports demonstrated that HO-1 has a cytoprotective role in glioma and provided evidence that HO-1 could be a potential therapeutic target in this cancer type [49]. Also, several groups showed that a decrease [49, 50] or

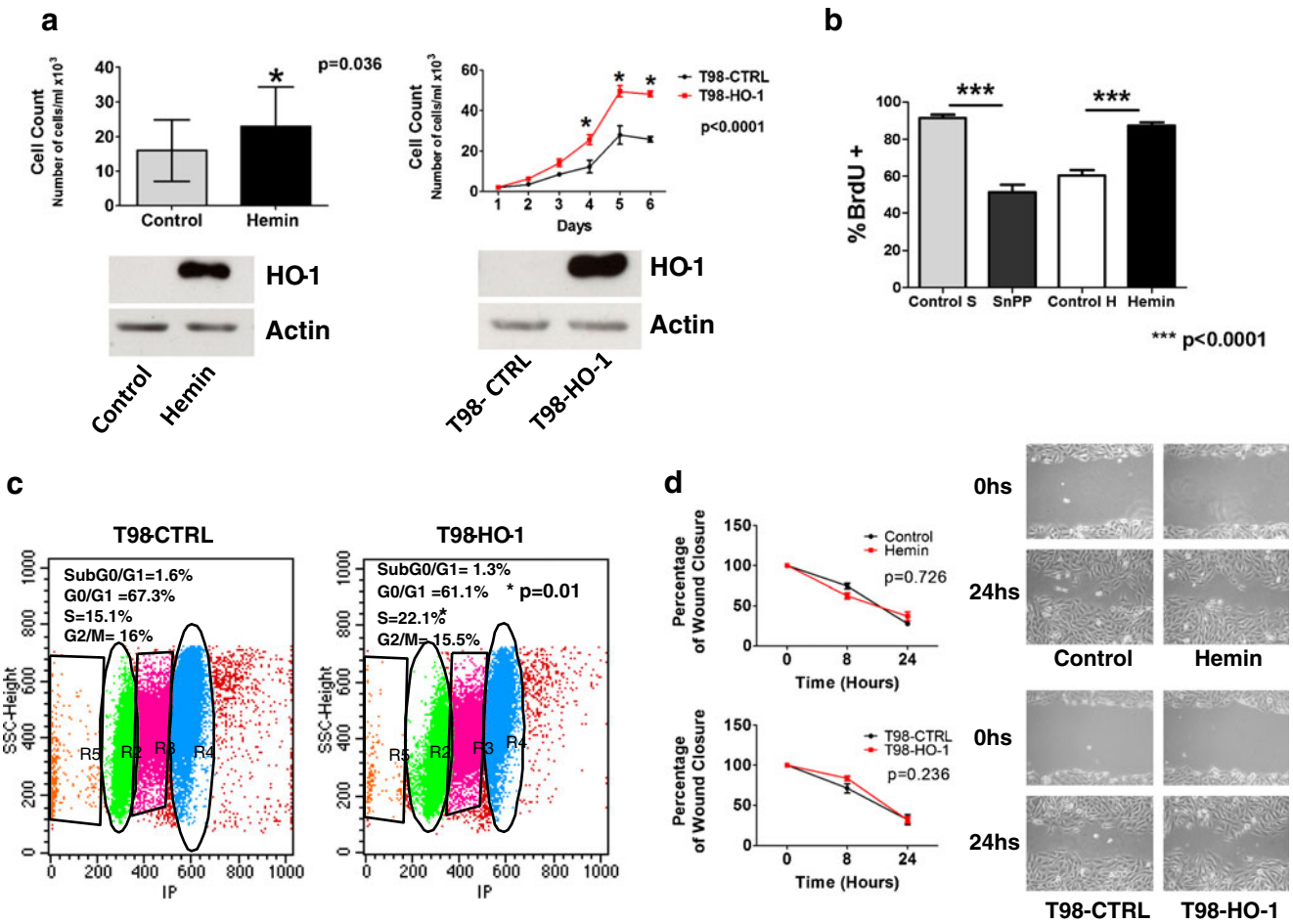


**Fig. 5** HO-1 modulation of glioma cell proliferation and migration. **a** T98G cells were treated with hemin 80 μM or vehicle for 48 h and cell count was performed. Additionally, T98G cells were transfected either with HO-1-overexpressing plasmid (*T98-HO-1*) or with control vector (*T98-CTRL*) and stable transfectants were selected and amplified, as described. Cell count was performed for 6 days. Shown *below* are the blots demonstrating HO-1 overexpression by either hemin or stable transfection (the absence of HO-1 expression in the control lines in comparison with the control lines of Fig. 1a (*lines 1* and *3*) is due to the short time of film exposition and different amount of protein loaded). The experiments were repeated twice and performed in quadruplicate. Shown is the mean±SE. **b** T98G cells were treated with hemin, SnPP, or vehicles for 72 h and BrdU incorporation was performed as described. **c** T98-HO-1 and T98-CTRL cells were stained with PI followed by flow cytometry in order to analyze the percentage of cells in the different phases of the cell cycle. **d** Wound closure assay in both hemin-treated cells (*above*) and T98-HO-1 and T98-CTRL ones (*below*) was performed. These experiments were carried out in triplicate and were repeated twice

an increase [51, 52] in HO-1 is necessary for the anticancer effects of many compounds on human glioma cells. All these reports point to a role of HO-1 in glial cell pathophysiology and suggest that HO-1 expression in these cell types might have a role in glioma progression and/or treatment, thus supporting our results of HO-1 expression by the glial cells within the tumor.

There are conflicting reports as to the role HO-1 plays in tumor initiation and progression since it has been demonstrated that HO-1 can play a role as a tumor-promoter molecule or have inhibitory effects on tumor progression [14, 18]. For example, in prostate cancer, HO-1 overexpression has been shown to reduce cellular proliferation and migration [53] and to negatively modulate the angiogenic switch [54], thereby exerting antitumoral effects. Contrariwise, HO-1 has been shown to stimulate the proliferation of melanoma, hepatoma, sarcoma, and pancreatic cancer cells, thus suggesting a permissive role of HO-1 in tumor growth [18].

In this sense, the study of HO-1 prognostic significance in human tumors is relevant, and again, the reports show contradictory results. For example, in bladder [55, 56] and lung cancer [57], HO-1 expression was significantly associated with recurrence and progression, whereas in tongue squamous cell carcinoma, low expression correlated with lymph node metastasis [58]; in colorectal cancer, the expression of HO-1 was associated with a longer survival time [59].

In relation to the role of HO-1 in glioma progression, we investigated the correlation of HO-1 expression with some clinicopathological parameters important in the prognosis of gliomas. Interestingly, we observed that the expression of HO-

1 was higher in all histological subtypes and all grades analyzed when compared to non-malignant brain tissue. No differences were observed among the various tumor grades, thus suggesting that since HO-1 expression increases significantly in low-grade glioma, no further increases are detected in higher-grade tumors. Importantly, HO-1 protein expression was associated with worse prognosis of grade II and III astrocytoma patients, and although this subgroup of astrocytomas was small, the results were corroborated at the mRNA level in univariate and multivariate analyses using the REMBRANDT data. Furthermore, the results demonstrating an increase in HO-1 protein in all glioma subtypes are also reflected at the mRNA level, as shown in the REMBRANDT database. Altogether, these results show that HO-1 is an independent prognostic factor and that its expression could be relevant in determining the malignant behavior of grade II and III astrocytomas.

The correlation of HO-1 with worse prognosis of grade II and III astrocytic tumors is in accordance with the results obtained in non-small cell lung cancer [57], prostate [60], and bladder cancer [58]. This association of HO-1 expression with astrocytoma patients' shorter survival is also in accordance with the results obtained in human and rat glioma cell lines, where cytoprotective and pro-tumoral effects of HO-1 have been demonstrated [49, 61–63]. Indeed, we have also demonstrated in this work that both pharmacological and genetic inductions of HO-1 in a human glioma cell line increase cell proliferation, thus supporting the results obtained in human specimens.

Since their initial discovery in 1968, HO-1 enzymes have been characterized as endoplasmic reticulum (ER)-associated proteins due to the abundant detection of HO activity in microsomal (104,000$g$) fractions. Recent studies have raised the possibility of the functional localization of HO-1 in other subcellular compartments besides the ER, including the nucleus and plasma membrane [18]. Therefore, we investigated whether nuclear localization could be observed in human glioma specimens. Indeed, in this work, we demonstrated HO-1 nuclear expression in some cells within the glioma tissues, and this observation was confirmed in the T98G cell line. Surprisingly, the number of cells showing nuclear expression of HO-1 was much higher in this cell line compared with tumor tissues (Fig. 1). Presumably, this difference is due to cell culture conditions. These results are consistent with documented studies in prostate cancer [30, 53, 64], NIH3T3 cell line [29], chronic myeloid leukemia [31], and with previous results from our laboratory obtained in head and neck squamous cell carcinoma [23]. In the present work, the HO-1 nuclear expression rates that we observed in glioma specimens did not show an association with tumor progression. However, the number of nuclear HO-1-expressing cells was relatively low, thus precluding a strong correlation analysis. Further research should be conducted to investigate whether this nuclear localization of HO-1 has a cause–effect relationship in gliomagenesis and/or progression.

In conclusion, our studies provide strong evidence of HO-1 overexpression in human gliomas compared with non-malignant samples. Furthermore, the expression of HO-1 was observed in tumor cells and was associated with a worse prognosis in patients with grade II and III astrocytoma. Preliminary analyses of the significance of HO-1 and its correlation with outcome in gliomas suggest that the enzyme might be involved in tumor cell proliferation. Altogether, these results point to a pro-tumoral role of HO-1 in glioma progression.

**Acknowledgments** This work was supported by grants from CONICET, ANPCyT and from the Technical Secretary of the Universidad Nacional del Sur. Gandini NA, Fermento ME, Andrés NC, Obiol DJ, and Salomón DG are recipients of a fellowship from CONICET.

**Conflict of interest** None.

## References

1. Demuth T, Berens ME. Molecular mechanisms of glioma cell migration and invasion. J Neurooncol. 2004;70:217–28.
2. Kotliarov Y, Kotliarova S, Charong N, Li A, Walling J, Aquilanti E, et al. Correlation analysis between single-nucleotide polymorphism and expression arrays in gliomas identifies potentially relevant target genes. Cancer Res. 2009;69:1596–603.
3. Shai R, Shi T, Kremen TJ, Horvath S, Liau LM, Cloughesy TF, et al. Gene expression profiling identifies molecular subtypes of gliomas. Oncogene. 2003;22:4918–23.
4. Ohgaki H. Genetic pathways to glioblastomas. Neuropathology. 2005;25:1–7.
5. Li A, Bozdag S, Kotliarov Y, Fine HA. GliomaPredict: a clinically useful tool for assigning glioma patients to specific molecular subtypes. BMC Med Inform Decis Mak. 2010;10:38. doi:10.1186/1472-6947-10-38.
6. Louis DN, Ohgaki H, Wiestler OD, Cavenee WK, Burger PC, Jouvet A, et al. The 2007 WHO classification of tumors of the central nervous system. Acta Neuropathol. 2007;114:97–109.
7. Ware ML, Berger MS, Binder DK. Molecular biology of glioma tumorigenesis. Histol Histopathol. 2003;18:207–16.
8. Reifenberger G, Collins VP. Pathology and molecular genetics of astrocytic gliomas. J Mol Med. 2004;82:656–70.
9. Huse JT, Holland EC. Targeting brain cancer: advances in the molecular pathology of malignant glioma and medulloblastoma. Nat Rev Cancer. 2010;10:319–31.
10. Haas-Kogan DA, Prados MD, Tihan T, Eberhard DA, Jelluma N, Arvold ND, et al. Epidermal growth factor receptor, protein kinase B/Akt, and glioma response to erlotinib. J Natl Cancer Inst. 2005;97:880–7.
11. Raizer JJ. HER1/EGFR tyrosine kinase inhibitors for the treatment of glioblastoma multiforme. J Neurooncol. 2005;74:77–86.
12. Tenhunen R, Marver HS, Schmid R. The enzymatic conversion of heme to bilirubin by microsomal heme oxygenase. Proc Natl Acad Sci U S A. 1968;61:748–55.
13. De Matteis F, Dawson SJ, Pons N, Pipino S. Bilirubin and uroporphyrinogen oxidation by induced cytochrome P4501A and cytochrome P4502B. Role of polyhalogenated biphenyls of different configuration. Biochem Pharmacol. 2002;63:615–24.

14. Jozkowicz A, Was H, Dulak J. Heme oxygenase-1 in tumors: is it a false friend? Antioxid Redox Signal. 2007;9:2099–117.
15. Otterbein LE, Bach FH, Alam J, Soares M, Tao Lu H, Wysk M, et al. Carbon monoxide has anti-inflammatory effects involving the mitogen-activated protein kinase pathway. Nat Med. 2000;6:422–8.
16. Snyder SH, Barañano DE. Heme oxygenase: a font of multiple messengers. Neuropsychopharmacology. 2001;25:294–8.
17. Maines MD, Gibbs PE. 30 some years of heme oxygenase: from a "molecular wrecking ball" to a "mesmerizing" trigger of cellular events. Biochem Biophys Res Commun. 2005;338:568–77.
18. Was H, Dulak J, Jozkowickz A. Heme oxygenase-1 in tumor biology and therapy. Curr Drug Targets. 2010;11:1551–70.
19. Dwyer BE, Nishimura RN, Lu SY. Differential expression of heme oxygenase-1 in cultured cortical neurons and astrocytes determined by the aid of a new heme oxygenase antibody. Response to oxidative stress. Brain Res Mol Brain Res. 1995;30:37–47.
20. Schipper HM. Heme oxygenase expression in human central nervous system disorders. Free Radic Biol Med. 2004;37:1995–2011.
21. Hanahan D, Weinberg RA. The hallmarks of cancer. Cell. 2000;100: 57–70.
22. Hanahan D, Weinberg RA. Hallmarks of cancer: the next generation. Cell. 2011;144:646–74.
23. Gandini NA, Fermento ME, Salomón DG, Blasco J, Patel V, Gutkind JS, et al. Nuclear localization of heme oxygenase-1 is associated with tumor progression of head and neck squamous cell carcinomas. Exp Mol Pathol. 2012;93:237–45.
24. Degese MS, Mendizabal JE, Gandini NA, Gutkind JS, Molinolo A, Hewitt SM, et al. Expression of heme oxygenase-1 in non-small cell lung cancer (NSCLC) and its correlation with clinical data. Lung Cancer. 2012;77:168–75.
25. Hara E, Takahashi K, Tominaga T, Kumabe T, Kayama T, Suzuki H, et al. Expression of heme oxygenase and inducible nitric oxide synthase mRNA in human brain tumors. Biochem Biophys Res Commun. 1996;224:153–8.
26. Deininger MH, Meyermann R, Trautmann K, Duffner F, Grote EH, Wickboldt J, et al. Heme oxygenase (HO)-1 expressing macrophages/microglial cells accumulates during oligodendroglioma progression. Brain Res. 2000;882:1–8.
27. El Andaloussi A, Lesniak MS. $CD4^+CD25^+FoxP3^+$ T-cell infiltration and heme oxygenase-1 expression correlate with tumor grade in human gliomas. J Neurooncol. 2007;83:145–52.
28. Nishie A, Ono M, Shono T, Fukushi J, Otsubo M, Onoue H, et al. Macrophage infiltration and heme oxygenase-1 expression correlate with angiogenesis in human gliomas. Clin Cancer Res. 1999;5:1107–13.
29. Lin Q, Weis S, Yang G, Weng YH, Helston R, Rish K, et al. Heme oxygenase-1 protein localizes to the nucleus and activates transcription factors important in oxidative stress. J Biol Chem. 2007;282:20621–33.
30. Sacca P, Meiss R, Casas G, Mazza O, Calvo JC, Navone N, et al. Nuclear translocation of haeme oxygenase-1 is associated to prostate cancer. Br J Cancer. 2007;97:1683–9.
31. Tibullo D, Barbagallo I, Giallongo C, La Cava P, Parrinello N, Vanella L, et al. Nuclear translocation of heme oxygenase-1 confers resistance to imatinib in chronic myeloid leukemia cells. Curr Pharm Des. 2013;19:2765–70.
32. Li Volti G, Ientile R, Abraham NG, Vanella A, Cannavò G, Mazza F, et al. Immunocytochemical localization and expression of heme oxygenase-1 in primary astroglial cell culture during differentiation: effect of glutamate. Biochem Biophys Res Commun. 2004;315:517–24.
33. Madhavan S, Zenklusen JC, Kotliarov Y, Sahni H, Fine HA, Buetow K. Rembrandt: helping personalized medicine become a reality through integrative translational research. Mol Cancer Res. 2009;7:157–67.
34. Greene FL. The American Joint Committee on Cancer: updating the strategies in cancer staging. Bull Am Coll Surg. 2002;87:13–5.
35. Facchinetti MM, Gandini NA, Fermento ME, Sterin-Speziale NB, Ji Y, Vyomesh Patel J, et al. The expression of sphingosine kinase-1 in head and neck carcinoma. Cells Tissues Organs. 2010;192:314–24.
36. Zlobec I, Steele R, Terracciano L, Jass JR, Lugli A. Selecting immunohistochemical cut-off scores for novel biomarkers of progression and survival in colorectal cancer. J Clin Pathol. 2007;60(10):1112–6.
37. Petit V, Boyer B, Lentz D, Turner CE, Thiery JP, Valles AM. Phosphorylation of tyrosine residues 31 and 118 on paxillin regulates cell migration through an association with CRK in NBT-II cells. J Cell Biol. 2000;148:957–70.
38. Schacter BA, Kurz P. Alterations in hepatic and splenic microsomal electron transport system components, drug metabolism, heme oxygenase activity, and cytochrome P-450 turnover in Murphy–Sturm lymphosarcoma-bearing rats. Cancer Res. 1982;42:3557–64.
39. Maines MD, Abrahamsson PA. Expression of heme oxygenase-1 (HSP32) in human prostate: normal, hyperplastic, and tumor tissue distribution. Urology. 1996;47:727–33.
40. Goodman AI, Choudhury M, daSilva JL, Schwartzman ML, Abraham NG. Overexpression of the heme oxygenase gene in renal cell carcinoma. Proc Soc for Exp Biol Med. 1997;214:54–61.
41. Doi K, Akaike T, Fujii S, Tanaka S, Ikebe N, Beppu T, et al. Induction of haem oxygenase-1 nitric oxide and ischaemia in experimental solid tumors and implications for tumor growth. Br J Cancer. 1999;80:1945–54.
42. Torisu-Itakura H, Furue M, Kuwano M, Ono M. Co-expression of thymidine phosphorylase and heme oxygenase-1 in macrophages in human malignant vertical growth melanomas. Jpn J Cancer Res. 2000;91:906–10.
43. McAllister SC, Hansen SG, Ruhl RA, Raggo CM, DeFilippis VR, Greenspan D, et al. Kaposi sarcoma-associated herpesvirus (KSHV) induces heme oxygenase-1 expression and activity in KSHV-infected endothelial cells. Blood. 2004;103:3465–73.
44. Berberat PO, Dambrauskas Z, Gulbinas A, Giese T, Giese N, Künzli B, et al. Inhibition of heme oxygenase-1 increases responsiveness of pancreatic cancer cells to anticancer treatment. Clin Cancer Res. 2005;11:3790–8.
45. Mayerhofer M, Florian S, Krauth MT, Aichberger KJ, Bilban M, Marculescu R, et al. Identification of heme oxygenase-1 as a novel BCR/ABL-dependent survival factor in chronic myeloid leukemia. Cancer Res. 2004;64:3148–54.
46. Chang KW, Lee TC, Yeh WI, Chung MY, Liu CJ, Chi LY, et al. Polymorphism in heme oxygenase-1 (HO-1) promoter is related to the risk of oral squamous cell carcinoma occurring on male areca chewers. Br J Cancer. 2004;91:1551–5.
47. Lee J, Lee SK, Lee BU, Lee HJ, Cho NP, Yoon JH, et al. Upregulation of heme oxygenase-1 in oral epithelial dysplasias. Int J Oral Maxillofac Surg. 2008;37:287–92.
48. Lee SS, Yang SF, Tsai CH, Chou MC, Chou MY, Chang YC. Upregulation of heme oxygenase-1 expression in areca-quid-chewing-associated oral squamous cell carcinoma. J Formos Med Assoc. 2008;107:355–63.
49. Liu Y, Liang Y, Zheng T, Yang G, Zhang X, Sun Z, et al. Inhibition of heme oxygenase-1 enhances anti-cancer effects of arsenic trioxide on glioma cells. J Neurooncol. 2011;104:449–58.
50. Chen CH, Chang YJ, Ku MS, Chung KT, Yang JT. Enhancement of temozolomide-induced apoptosis by valproic acid in human glioma cell lines through redox regulation. J Mol Med (Berl). 2011;89:303–15.
51. Long J, Manchandia T, Ban K, Gao S, Miller C, Chandra J. Adaphostin cytoxicity in glioblastoma cells is ROS-dependent and is accompanied by upregulation of heme oxygenase-1. Cancer Chemother Pharmacol. 2007;59:527–635.
52. Asharani PV, Hande MP, Valiyaveettil S. Anti-proliferative activity of silver nanoparticles. BMC Cell Biol. 2009;10:65.
53. Gueron G, De Siervi A, Ferrando M, Salierno M, De Luca P, Elguero B, et al. Critical role of endogenous heme oxygenase 1 as a tuner of the invasive potential of prostate cancer cells. Mol Cancer Res. 2009;7:1745–55. doi:10.1158/1541-7786.MCR-08-0325.

54. Ferrando M, Gueron G, Elguero B, Giudice J, Salles A, Leskow FC, et al. Heme oxygenase 1 (HO-1) challenges the angiogenic switch in prostate cancer. Angiogenesis. 2011;14(4):467–79.
55. Miyake M, Fujimoto K, Anai S, Ohnishi S, Nakai Y, Inoue T, et al. Clinical significance of heme oxygenase-1 expression in non-muscle-invasive bladder cancer. Urol Int. 2010;85:355–63. doi:10.1159/000317785.
56. Yim MS, Ha YS, Kim IY, Yun SJ, Choi YH, Kim WJ. HMOX1 is an important prognostic indicator of nonmuscle invasive bladder cancer recurrence and progression. J Urol. 2011;185:701–5.
57. Tsai JR, Wang HM, Liu PL, Chen YH, Yang MC, Chou SH, et al. High expression of heme oxygenase-1 is associated with tumor invasiveness and poor clinical outcome in non-small cell lung cancer patients. Cell Oncol (Dordr). 2012;35:461–71.
58. Yanagawa T, Omura K, Harada H, Nakaso K, Iwasa S, Koyama Y, et al. Heme oxygenase-1 expression predicts cervical lymph node metastasis of tongue squamous cell carcinomas. Oral Oncol. 2004;40:21–7.
59. Becker JC, Fukui H, Imai Y, Sekikawa A, Kimura T, Yamagishi H, et al. Colonic expression of heme oxygenase-1 is associated with a better long-term survival in patients with colorectal cancer. Scand J Gastroenterol. 2007;42:852–8.
60. Li Y, Su J, DingZhang X, Zhang J, Yoshimoto M, Liu S, et al. PTEN deletion and heme oxygenase-1 overexpression cooperate in prostate cancer progression and are associated with adverse clinical outcome. J Pathol. 2011;224:90–100. doi:10.1002/path.2855.
61. Al-Owais MM, Scragg JL, Dallas ML, Boycott HE, Warburton P, Chakrabarty A, et al. Carbon monoxide mediates the anti-apoptotic effects of heme oxygenase-1 in medulloblastoma DAOY cells via $K^+$ channel inhibition. J Biol Chem. 2012;287:24754–64. doi:10.1074/jbc.M112.357012.
62. Lu TH, Pepe JA, Gildemeister OS, Tyrrell RM, Bonkovsky HL. Regulation of expression of the human heme oxygenase-1 gene in transfected chick embryo liver cell cultures. Biochim Biophys Acta. 1997;1352:293–302.
63. Pan HC, Yang CN, Hung YW, Lee WJ, Tien HR, Shen CC, et al. Reciprocal modulation of C/EBPα and C/EBPβ by IL-13 in activated microglia prevents neuronal death. Eur J Immunol. 2013. doi:10.1002/eji.201343301.
64. Birrane G, Li H, Yang S, Tachado SD, Seng S. Cigarette smoke induces nuclear translocation of heme oxygenase 1 (HO-1) in prostate cancer cells: nuclear HO-1 promotes vascular endothelial growth factor secretion. Int J Oncol. 2013;42:1919–28. doi:10.3892/ijo.2013.1910.